haematologica
Journal of the Ferrata Storti Foundation

Factor VIII promotes angiogenesis and vessel stability regulating extracellular matrix proteins

by Cristina Olgasi, Alessia Cucci, Ivan Molineris , Simone Assanelli, Francesca Anselmi, Chiara Borsotti, Chiara Sgromo, Andrea Lauria, Simone Merlin, Gillian E. Walker, Salvatore Oliviero, and Antonia Follenzi

Received: January 22, 2024.
Accepted: May 23, 2024.

Citation: Cristina Olgasi, Alessia Cucci, Ivan Molineris , Simone Assanelli, Francesca Anselmi, Chiara Borsotti, Chiara Sgromo, Andrea Lauria, Simone Merlin, Gillian E. Walker, Salvatore Oliviero, and Antonia Follenzi. Factor VIII promotes angiogenesis and vessel stability regulating extracellular matrix proteins.
Haematologica. 2024 June 6. doi: 10.3324/haematol.2024.285089 [Epub ahead of print]

Factor VIII promotes angiogenesis and vessel stability regulating extracellular matrix proteins

Cristina Olgasi[1*], Alessia Cucci[2*], Ivan Molineris[3,4*], Simone Assanelli[2*], Francesca Anselmi[3,4], Chiara Borsotti[2], Chiara Sgromo[2], Andrea Lauria[3,4], Simone Merlin[2], Gillian E. Walker[2], Salvatore Oliviero[3,4#] and Antonia Follenzi[2,5#]

1Department of Translational Medicine, Università degli Studi del Piemonte Orientale, Novara, Italy.

2Department of Health Sciences, Università degli Studi del Piemonte Orientale, Novara, Italy.

3Università degli Studi di Torino, Torino, Italy.

4Italian Institute for Genomic Medicine (IIGM), Candiolo, Italy.

5Dipartimento Attività Integrate Ricerca Innovazione, Azienda Ospedaliero-Universitaria SS. Antonio e Biagio e C. Arrigo, Alessandria, Italy.

CO, AC, IM and SA contributed equally as co-first authors
SO and AF contributed equally as senior authors

Corresponding authors: Prof. Antonia Follenzi, MD, PhD antonia.follenzi@med.uniupo.it;

Prof. Salvatore Oliviero, PhD salvatore.oliviero@unito.it

Acknowledgments

The authors thank Roberta Annamaria Cirsmaru for lentiviral vector production. The authors would like to thank prof. Guido Serini, prof. Livio Trusolino, prof. Federico Mingozzi, and prof. Anna Randi for the helpful discussions and Dr. Marcello Arsura for the scientific English revision.

Authors Contribution

CO, AC and SA designed and performed the experiments and analyzed the data. CS, GW and SM performed the experiments and analyzed the data. CB conducted the in vivo studies. IM, FA and AL designed and performed RNAseq transcriptomic analysis. AF conceived the study. AF and SO generated fundings, analyzed data and supervised the project. CO, AC, SA, AF and SO wrote the manuscript that was revised by all authors and approved the final version.

Fundings

AF was supported by Telethon grant No. GGP19201, in part by Vanguard grant No. 874700, by Ministero della Sanità RF-2018-12366471 and by CSP - Compagnia San PaoloTrapezio No 68155. SO was supported by Telethon grant No. GGP19201 and by AIRC IG 2022ID 27155. CO was supported by Bando per la Ricerca Roche, Ministero della Sanità GR-2018-12366399. CB was supported by Fondazione Cariplo grant No. 2018-0253.

Disclosures

Patent application of AF: international application number PCT/IB2017/054574. Title: METHOD FOR INDUCING AND DIFFERENTIATING PLURIPOTENT STEM CELLS AND USES THEREOF

Data sharing statement: For original data, please contact the corresponding authors.

Factor VIII (FVIII) is a crucial coagulation cofactor and mutations in *F8* gene lead to hemophilia A (HA). FVIII reduced activity or absence results in bleeding episodes, which can occur either spontaneously or secondary to trauma.[1] To date, there is no definitive cure for HA. The standard therapy involves prophylaxis either with replacement products, as recombinant human FVIII (rhFVIII), or non-substitutive treatment as a gold standard for the severe cases to prevent bleeding events.[2] Besides general bleeding complications, HA patients have been recently reported to have an attenuated microvascular endothelial functionality and an altered plasmatic collagen level, suggesting a dysfunction in endothelial cells (ECs)[3,4]. Endothelial dysfunction in these patients is evidenced by decreased flow-mediated dilation (FMD) and reduced hyperemic LSE (VTI) compared to healthy controls.[5,6] Furthermore, studies involving FVIII-deficient mice have revealed substantial alterations in joint vascular remodeling and increased synovial vascular permeability following hemarthrosis induction[7–9]. This suggests a non-physiological angiogenic response that may exacerbate the severity of the bleeding episodes and the vulnerability of the vascular system in FVIII absence. Overall, these findings suggest that hemorrhagic events in HA patients might result not only from impaired clotting but also from vascular abnormalities, indicating the development of an endothelial dysfunction in these patients. Extensive research has established that ECs are a primary source of FVIII, particularly liver sinusoidal ECs (LSECs)[10] while the specific role of FVIII in EC physiology remains poorly described. Therefore, we investigated the role of FVIII in EC function using blood outgrowth endothelial cells (BOECs), an optimal model for studying EC biology and for the development of therapeutic cell and gene therapy strategies.[11] In particular, BOECs obtained from severe HA patients (HA-BOECs) displayed defective endothelial functionality, which was reversed by FVIII treatment. Consistent with this, FVIII was also *in vivo* required for proper angiogenesis and preservation of vessel integrity in a HA mouse model. Mechanistically, we found that FVIII induces an EC signaling activating the focal adhesion kinase (FAK)/ SRC proto-oncogene (Src) pathway regulating the expression of genes related to the

basement membrane and the extracellular matrix (ECM). Overall, these data identify FVIII as a player in the control of vessel stability.

First, we demonstrated that, when cultured on Matrigel®, HA-BOECs formed a sparse and incomplete vascular network compared to BOECs derived from healthy donors (C-BOECs) that developed a complete and stable vascular network (Figure 1A). The functional impairment of HA-BOECs was also evident in migration (Figure 1A) and permeability (Figure 1A) assays. Notably, HA-BOECs transduced with a lentiviral vector (LV) carrying the *F8* transgene (LV-FVIII) (LV-FVIII HA-BOECs) showed a significantly improved tubule network formation, migration, and permeability, akin to the results seen in C-BOECs (Figure 1A). To determine whether acute treatment of BOECs with rhFVIII would also improve some EC functions, we challenged both C-BOECs and HA-BOECs with several doses of rhFVIII (5 IU/ml, 1 IU/ml, 0.5 IU/ml, 0.2 IU/ml and 0.1 IU/ml). Remarkably, while HA-BOECs evidenced marked improvements in tubule formation, migration, and permeability starting from a rhFVIII concentration of 0.2 IU/ml, C-BOECs showed no further increase in functionality following rhFVIII treatment (Figure S1A-D), suggesting that the endogenous FVIII secretion by BOECs themselves is sufficient to guarantee their activity.

Therefore, we hypothesized that FVIII could trigger a signaling pathway in ECs which modulates angiogenesis, their migration and permeability. Indeed, we found that rhFVIII induced the phosphorylation of FAK and Src along with the downstream targets AKT, mTOR, and p38, but not ERK (Figure 1B and C). This signaling cascade is widely recognized to control EC function upon several stimuli. However, the lack of Vascular Endothelial Growth Factor Receptor 2 (VEGFR2) and ERK phosphorylation upon rhFVIII stimulation (Figure 1D) suggests that FVIII induces a different pathway compared to the classical one triggered by VEGF. Moreover, by comparing HA- versus C-BOECs, it was evident that the above-mentioned signaling pathway is activated in untreated C-BOECs (Figure S1E), suggesting that FVIII can act as an autocrine factor.

To confirm that FVIII controls EC functions through FAK activation, we performed tubulogenesis, migration, and permeability assays on HA-BOECs treated first with Defactinib, an inhibitor of FAK

(FAKi), and then exposed to rhFVIII. We observed that FAKi treatment significantly disrupted the FVIII-dependent response of HA-BOECs (Figure 1E). When transferred *in vivo* in an immunodeficient mouse model of HA, NOD-*scid* IL2Rg^{null} (NSG) (NSG-HA), C-BOECs expressing green fluorescent protein (GFP) and embedded in Matrigel® plugs, formed well-organized vascular structures while HA-BOECs exhibited a significant deficiency in vessel formation (Figure 2A). This impairment was effectively rescued by either transducing HA-BOECs with LV-FVIII or supplementing rhFVIII into the Matrigel® plugs (Figure 2A). Vessel density and diameter quantification confirmed that both LV-FVIII transduction and rhFVIII treatment markedly improved the ability of HA-BOECs to form well-organized vessels in Matrigel® plugs implanted in HA mice (Figure 2B).

To further investigate *in vivo* the role of FVIII in angiogenesis, we assessed the vessel formation potential of murine ECs in adult NSG *versus* (*vs*) NSG-HA mice implanted intradermally with Matrigel® plugs. In NSG mice, ECs, identified by the murine CD31 expression, built a well-organized vessel network, stabilized by alpha Smooth Muscle Actin (αSMA) pericytes (Figure 2C). Conversely, NSG-HA ECs formed smaller and more disorganized vessels. The injection of NSG-HA mice with either $5x10^8$ Transduction Units/mouse of LV-FVIII or 2 IU of rhFVIII (every two days) promoted the formation of larger and more stable vessels (Figure 2C). The quantification of their density and diameter further indicated that FVIII contributes to *in vivo* angiogenesis in FVIII-deficient mice (Figure 2D).

Vessel permeability was *in vivo* evaluated by intravenous injection of Evans blue, an albumin-binding dye, into NSG *v*s NSG-HA mice. Under physiological conditions the endothelium is impermeable to albumin, restricting Evans blue within the blood vessels, while increased EC permeability of NSG-HA mice was demonstrated by Evans blue extravasation into the interstitial tissue (Figure 2E). Intriguingly, both LV-FVIII and rhFVIII (4 IU every two days for 20 days) showed a marked reduction in dye extravasation (Figure 2E). Taken together, these results indicate that FVIII plays a crucial role in angiogenesis and in vessel integrity maintenance.

To investigate the impact of FVIII on the EC transcriptome, we performed RNAseq comparing HA- to C-BOECs, and LV-FVIII HA to HA-BOECs (Figure 3A). The volcano plot revealed that 215 genes were upregulated and 155 genes downmodulated in HA- *vs* C-BOECs (Figure 3B), including among the latter predominantly genes involved in ECM composition, such as collagen4a1 (*COL4A1*), nidogen2 (*NID2*), fibulin1 (*FBN1*), and peroxidasin (*PXDN*). Importantly, the expression level of most of these genes was significantly restored when FVIII was reintroduced into HA-BOECs (Figure 3A and C). Supporting our *in vitro* and *in vivo* findings, gene set enrichment analysis (GSEA) and gene ontology (GO) process analysis of differentially expressed genes (DEGs), identified pathways corresponding to vascular development, cell migration, regulation of cell adhesion, extracellular matrix organization, and integrin cell surface interactions. These pathways were downregulated in HA- *vs* C-BOECs and rescued by LV-FVIII transduction (Figure S2 A-B).

Finally, to gain deeper mechanistic insights of FVIII role in ECs we focused on NID2, a glycoprotein critical for endothelial basement membrane stability, since it was one of the most significantly downregulated gene in HA- *vs* C-BOECs and rescued by LV-mediated transduction of FVIII (Figure 3D-E). Importantly, FAK inhibition in ECs treated with rhFVIII prevented FVIII-induced increase of NID2 (Figure 3D right panel). We performed a complementation assay by ectopically expressing NID2 in HA-BOECs (Figure S3A), which led to the formation of stable tubule networks in Matrigel®, enhanced their migration capabilities and, remarkably, restored barrier integrity to levels comparable to those seen in C-BOECs (Figure S3B). NID2 knockdown by shRNA in C-BOECs (Figure S3C) significantly impaired EC tubulogenesis, migration and increased EC permeability (Figure S3D). Treatment with rhFVIII failed to restore the impaired functions in these NID2-deficient ECs (Figure S3D), confirming that NID2 is required for FVIII-mediated regulation of fundamental EC activity.

Taken together, our findings indicate that BOECs from HA patients own an impaired endothelial functionality, which is compensated by FVIII treatment.

One of the main FVIII partner in coagulation is von Willebrand factor (VWF), reported to exert both pro and anti-angiogenic effects. Indeed, reduced VWF expression in ECs increase their migration, proliferation, and angiogenesis *in vitro*. In a similar way, mice lacking VWF display an elevated vessel formation and a large vascular network in the ear.[12] Although its mechanism of action in regulating vessel formation is yet not fully understood, VWF has been suggested to bind and recruit several angiogenic growth factors to the cell membrane thanks to its heparin binding domain.[13] Interestingly, ECs lacking FVIII display the opposite behavior showing an impaired functionality. However, the mechanism of FVIII/VWF regulation in ECs biology requires further investigation.

Through the activation of the FAK/Src pathway, FVIII regulates the expression of genes related to the ECM structure, which is known to play a critical role in maintaining the integrity of the blood vessel structure, regulating EC migration and angiogenesis, and the formation of new blood vessels.[14,15] The link found here between FVIII and regulation of ECM genes agrees with the recent clinical findings reporting the reduction of plasmatic collagen level during hemarthrosis[8] and the elevated plasma levels of collagen XVIII in HA patients correlating with higher annual bleeding rates.[4] This evidence from the literature and our findings support the hypothesis that HA ECs exhibit significant deficit in ECM components , which can be mitigated by FVIII treatment. Moreover, it has been previously shown that NID2 is crucial for endothelial basement membrane integrity, largely due to its interaction with collagen IV, laminins, and perlecan. Recent studies have further identified the role of NID2 in regulating the EC phenotype, revealing its significant impact on ECM organization.[16,17] Thus, the observed reduction in NID2 expression in ECs isolated from severe HA patients may contribute to ECM impairment. Our results suggest that FVIII replacement therapy is not only fundamental to treat coagulation problems, but it might be helpful in maintaining the vascular integrity of HA patients by targeting several genes, such as NID2, involved in the ECM stability.

From a clinical standpoint, these findings suggest that FVIII replacement therapy for HA patients could offer benefits that go beyond the bleeding prevention, such as preservation of vascular health and resilience. This new perspective on FVIII functions paves the way for future research aimed at developing more multidisciplinary approaches for treating HA, targeting both coagulation deficiencies and vascular stability.

References

1. Bolton-Maggs PHB, Pasi KJ. Haemophilias A and B. Lancet. 2003;361(9371):1801-1809
2. Collins PW, Blanchette VS, Fischer K, et al. Break-through bleeding in relation to predicted factor VIII levels in patients receiving prophylactic treatment for severe hemophilia A. J Thromb Haemost. 2009;7(3):413-420.
3. Sartori MT, Bilora F, Zanon E, et al. Endothelial dysfunction in haemophilia patients. Haemophilia. 2008;14(5):1055-1062.
4. Kjeld NG, Hua B, Karsdal MA, Sun S, Manon-Jensen T. The endothelial specific isoform of type XVIII collagen correlates to annual bleeding rate in haemophilia patients. PLoS One. 2018;13(1):e0190375.
5. Biere-Rafi S, Tuinenburg A, Haak BW, et al. Factor VIII deficiency does not protect against atherosclerosis. J Thromb Haemost. 2012;10(1):30-37.
6. Sun H, Yang M, Fung M, et al. Adult males with haemophilia have a different macrovascular and microvascular endothelial function profile compared with healthy controls. Haemophilia. 2017;23(5):777-783.
7. Cooke EJ, Zhou JY, Wyseure T, et al. Vascular Permeability and Remodelling Coincide with Inflammatory and Reparative Processes after Joint Bleeding in Factor VIII-Deficient Mice. Thromb Haemost. 2018;118(6):1036-1047.
8. Gopal S, Barnes RFW, Cooke EJ, et al. Systemic vascular basement membrane markers linked to synovial vascular remodeling are biomarkers of hemarthrosis in patients with hemophilia. J Thromb Haemost. 2021;19(5):1200-1211.
9. Cooke EJ, Wyseure T, Zhou JY, et al. Mechanisms of vascular permeability and remodeling associated with hemarthrosis in factor VIII-deficient mice. J Thromb Haemost. 2019;17(11):1815-1826.

10. Follenzi A, Benten D, Novikoff P, Faulkner L, Raut S, Gupta S. Transplanted endothelial cells repopulate the liver endothelium and correct the phenotype of hemophilia A mice. J Clin Invest. 2008;118(3):935-945.
11. Olgasi C, Borsotti C, Merlin S, et al. Efficient and safe correction of hemophilia A by lentiviral vector-transduced BOECs in an implantable device. Mol Ther Methods Clin Dev. 2021;23:551-566.
12. Randi AM, Smith KE, Castaman G. von Willebrand factor regulation of blood vessel formation. Blood. 2018;132(2):132-140.
13. Ishihara J, Ishihara A, Starke RD, et al. The heparin binding domain of von Willebrand factor binds to growth factors and promotes angiogenesis in wound healing. Blood. 2019;133(24):2559-2569.
14. Witjas FMR, van den Berg BM, van den Berg CW, Engelse MA, Rabelink TJ. Concise Review: The Endothelial Cell Extracellular Matrix Regulates Tissue Homeostasis and Repair. Stem Cells Transl Med. 2019;8(4):375-382.
15. Davis GE, Senger DR. Endothelial extracellular matrix: Biosynthesis, remodeling, and functions during vascular morphogenesis and neovessel stabilization. Circ Res. 2005;97(11):1093-1107.
16. Mao C, Ma Z, Jia Y, et al. Nidogen-2 Maintains the Contractile Phenotype of Vascular Smooth Muscle Cells and Prevents Neointima Formation via Bridging Jagged1-Notch3 Signaling. Circulation. 2021;144(15):1244-1261.
17. Chen Y, Mao C, Gu R, et al. Nidogen-2 is a Novel Endogenous Ligand of LGR4 to Inhibit Vascular Calcification. Circ Res. 2022;131(12):1037-1054.

Figure Legend

Figure 1. Factor VIII (FVIII) restores the defective functionality of hemophilia A Blood Outgrowth Endothelial Cells (HA-BOECs) through focal adhesion kinase (FAK)/ SRC proto-oncogene (Src) pathway involvement. A) Tubulogenic assay. Quantitative analysis of the number of nodes, junctions, branches, and total length of tubule networks using control (C)-BOECs (n=4), HA-BOECs (n=4), or HA-BOECs transduced with a lentiviral vector (LV) carrying the *F8* transgene (LV-FVIII HA-BOECs) (n=4). $5x10^4$ BOECs were placed on top of the Matrigel® and incubated overnight. ImageJ Angiogenesis software was used to quantify the number of nodes, junctions, branches, and total length of acquired images. Migration assay. Indirect measurement of cell migration through crystal violet staining elution of BOECs. BOECs were plated into the upper compartment of 8-μm pore size Transwell at a density of 10^5 cells per well in serum-free medium, while the lower compartment was filled with complete medium and incubated overnight. Migrated cells were stained with crystal violet that was eluted with acetic acid and quantified using Victor Spectrophotometer at 590 nm. Permeability assay. Permeability was measured by the extravasation of FITC-dextran across a monolayer of BOECs ($8x10^4$ cells/well) cultured on 0.1% gelatin coated Transwell (3 μm pore) until confluence was reached. At the end of the culture, 5 μg/ml of FITC-conjugated 40-kDa dextran was added to the upper chamber and the fluorescence of the lower chamber was measured in the medium using Victor Spectrophotometer (490 nm (excitation)/520 nm (emission)). Fluorescence readings were normalized to dextran permeability in Transwell inserts without cells. **B)** Western blot analysis of whole cell lysate (WCL) from HA-BOECs treated for 15 min with or without 1 IU/ml of B-domain-deleted rhFVIII and stained with antibodies against pFAK, total FAK, pSrc, total Src, pAKT, total AKT, pmTOR, total mTOR, pp38, total p38, pERK, and total ERK. Tubulin was used as a loading control. **C)** Quantification of increased phosphorylation of FAK, Src, AKT, mTOR, and p38 expressed as fold change relative to untreated control. **D)** Western blot analysis of WCL from HA-BOECs incubated for 15 min in the presence or absence of rhFVIII (1 IU/ml) or rhVEGF (50 ng/ml) and stained with antibody against phosphor Vascular Endothelial Growth Factor Receptor 2 (VEGFR2) and pERK. Tubulin was used as a loading control. **E)** Quantitative analysis of the number of nodes, junctions, branches, and total length of tubule networks performed on untreated or 1 μM FAK inhibitor (FAKi)-treated HA-BOECs. All cells were incubated in the presence or absence of 1 IU/mL of B-domain-deleted rhFVIII overnight. Indirect measurement of cell migration by elution of crystal violet staining in HA-BOECs. Permeability assay results calculated on the extravasation of FITC-dextran through an intact monolayer of BOECs. Data in **A,** and **E** are expressed as mean ± SD. Statistical analysis was performed by one-way ANOVA test (****$p < 0.0001$; ***$p < 0.001$; **$p < 0.01$; *$p < 0.05$).

Figure 2. Factor VIII (FVIII) boosts the *in vivo* angiogenic potential of endothelial cells and reduces the impaired vessel permeability in hemophilia A (HA) mice. A) Immunofluorescence analysis conducted on Matrigel® plugs to detect GFP+ control (C-) blood outgrowth endothelial cells (BOECs), hemophilia A (HA-BOECs), HA-BOECs transduced with a lentiviral vector (LV) carrying the *F8* transgene (LV-FVIII HA-BOECs) and HA-BOECs treated with B-domain-deleted rhFVIII. These were assessed for vessel formation within Matrigel® plugs transferred intradermally in NOD-*scid* $IL2Rg^{null}$ (NSG) (NSG-HA) mice (9 animals for each condition). Matrigel® plugs with cells were prepared by re-suspending $2x10^6$ BOECs in Matrigel®. The mix was implanted intradermally in 8-week-old NSG or NSG-HA mice. For FVIII stimulation, 3 IU/ml of B-domain-deleted rhFVIII was added to Matrigel® and 2 IU of rhFVIII were injected within the Matrigel® plug every 2 days. After 10 days, the plugs were removed, fixed, and embedded in Killik OCT for histological analysis. **B)** Quantification of vessel density in the transplanted plugs and measurement of vessel diameter of samples described in **A**. **C)** Immunofluorescence staining showing murine CD31 (red) and αSMA (green) on vessels formed within Matrigel® plug harvested from 8 week old NSG mice (n=6), NSG-HA mice (n=6), NSG-HA mice injected with LV-FVIII (n=3), and NSG-HA mice treated *in situ* with rhFVIII (n=6). Scale bar = 100 μm. For FVIII stimulation, 3 IU/ml of B-domain-deleted rhFVIII was added to Matrigel® and 2 IU of rhFVIII were injected within the Matrigel® plug every 2 days. After 10 days, the plugs were removed, fixed, and embedded in Killik OCT for histological analysis. **D)** Vessel density quantification in Matrigel® plugs and measurement of vessel diameter in Matrigel® plugs of the samples described in **C**. **E)** Representative images showcasing Evans blue dye extravasation in the interstitial tissue of 8-week-old NSG, NSG-HA mice, NSG-HA mice injected with LV- FVIII and NSG-HA

treated with rhFVIII. The total number of animals used for each condition was 6 except for NSG-HA mice injected with LV- FVIII, where 4 mice were used. For FVIII delivery, 4 IU/mice of B-domain deleted rhFVIII were tail vein injected every 2 days for 20 days. NSG-HA mice were also tail vein injected with $5x10^8$ transducing unit (TU)/ mouse of LV-FVIII. At the end of the experiment, Evans Blue solution was injected into the tail vein. After 15 min, mice were killed, and the extravasation was visualized in the interstitial space under the skin of the mice. Data in **B** and **D** are expressed as mean ± SD. Each dot represents the quantification of 1 image. Scale bar=100µm or 50µm. Statistical analysis was performed by one-way ANOVA test (****$p < 0.0001$). Animal studies were approved by the Animal Care and Use Committee at UPO (Italian Health Ministry Authorization nos. 492/2016-PR and DBO64.5).

Figure 3. Factor VIII (FVIII) regulates the expression of genes related to extracellular matrix such as nidogen 2 (*NID2*). A) Heatmap showing the expression pattern of genes modulated by FVIII. Upper panel showing upregulated genes in HA-BOECs *vs* C-BOECs and rescued in LV-FVIII HA-BOECs and *vice versa* in the lower panel. **B -C)** Volcano plot showing differentially expressed genes (DEGs) in hemophilia A (HA-) *versus* (*vs*) control (C-) blood outgrowth endothelial cells (BOECs) (**A**) and HA-BOECs transduced with a lentiviral vector (LV) carrying the *F8* transgene (LV-FVIII HA-BOECs) *vs* HA-BOECs (**B**). Genes are classified as up-regulated if they have a log fold change > 1 and *p*-value < 0.01, and as down-regulated if they have a log fold change < -1 and *p*-value < 0.01. **D)** Left panel: Western blot analysis of NID2 expression levels in C-BOECs (n=4), HA-BOECs (n=3), and LV-FVIII HA-BOECs (n=3). An anti-vinculin antibody was used to confirm equal loading. Right panel: Western blot analysis of NID2 expression in HA-BOECs treated or not with B-domain-deleted rhFVIII in the presence or absence of 1 µM Defactinib (FAK inihibitor) for 48 h. An anti-tubulin antibody was used to confirm equal loading. **E)** Genome browser view showing the average RNAseq signal profile of the *NID2* gene in C-BOECs (n=4), HA-BOECs (n=3), and LV-FVIII HA-BOECs (n=3). RNAseq was performed in the Illumina sequencer NextSeq 500. Sequencing reads were aligned to human reference genome (version GRCh38.p13) using STAR v2.7.7a0 [5] (with parameters –outFilterMismatchNmax 999 –outFilterMismatchNoverLmax 0.04) and providing a list of known splice sites extracted from GENCODE comprehensive annotation (version 32). Expression counts were next analyzed using the edgeR package.

Figure 1

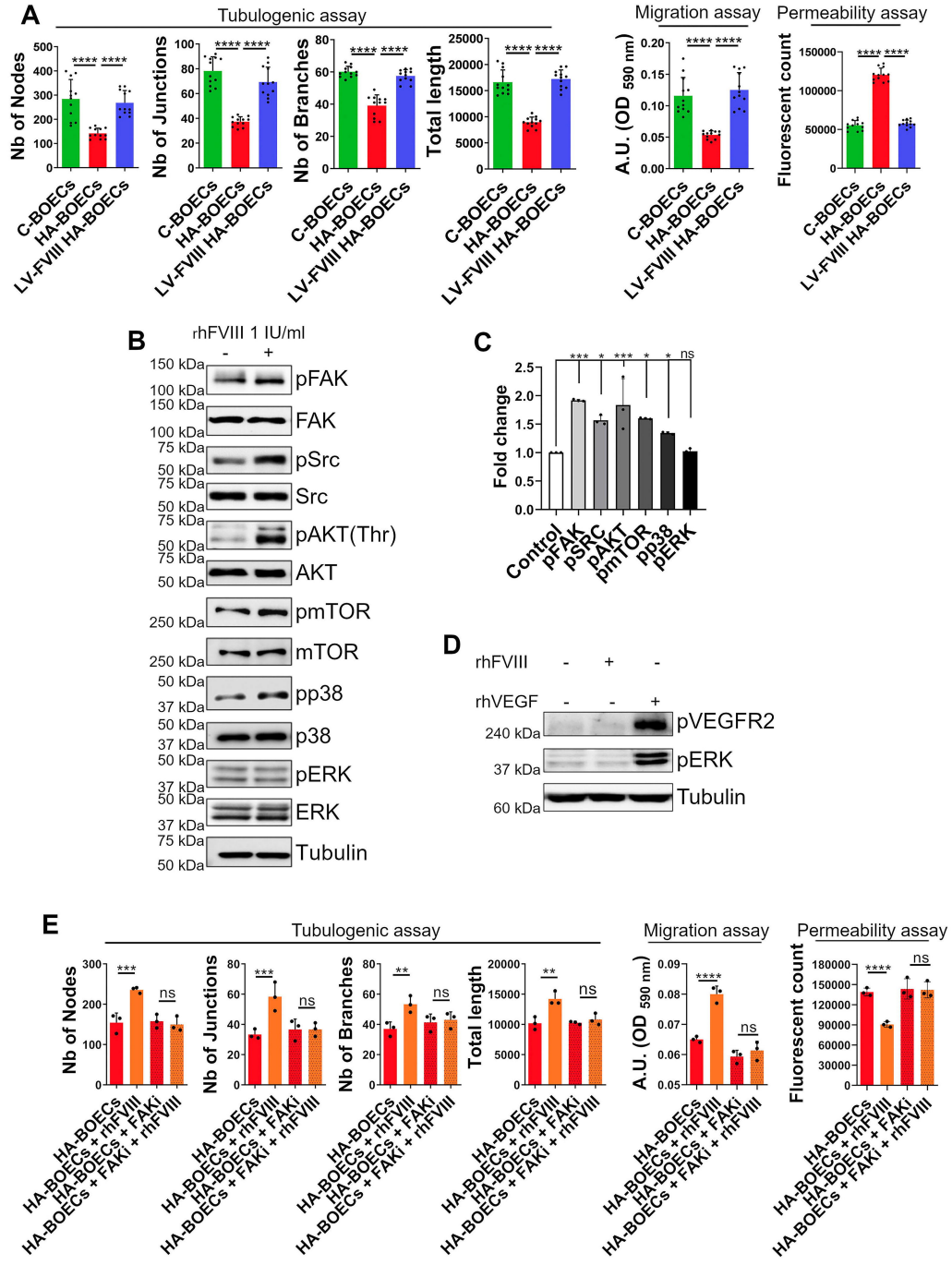
A
Tubulogenic assay
Migration assay
Permeability assay
Nb of Nodes
Nb of Junctions
Nb of Branches
Total length
A.U. (OD 590 nm)
Fluorescent count
C-BOECs
HA-BOECs
LV-FVIII HA-BOECs
B
rhFVIII 1 IU/ml
pFAK
FAK
pSrc
Src
pAKT(Thr)
AKT
pmTOR
mTOR
pp38
p38
pERK
ERK
Tubulin
C
Fold change
Control
pFAK
pSRC
pAKT
pmTOR
pp38
pERK
D
rhFVIII
rhVEGF
pVEGFR2
pERK
Tubulin
E
Tubulogenic assay
Migration assay
Permeability assay
HA-BOECs
HA-BOECs + rhFVIII
HA-BOECs + FAKi
HA-BOECs + FAKi + rhFVIII

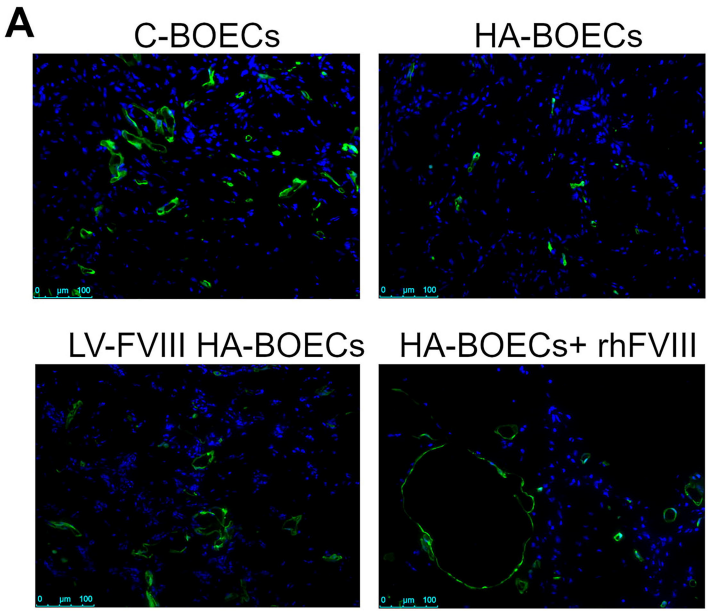
A
C-BOECs
HA-BOECs
LV-FVIII HA-BOECs
HA-BOECs+ rhFVIII

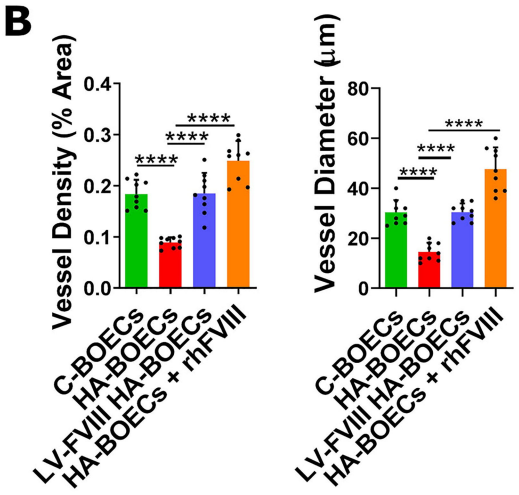
B
Vessel Density (% Area)
Vessel Diameter (µm)
C-BOECs
HA-BOECs
LV-FVIII HA-BOECs
HA-BOECs + rhFVIII
****

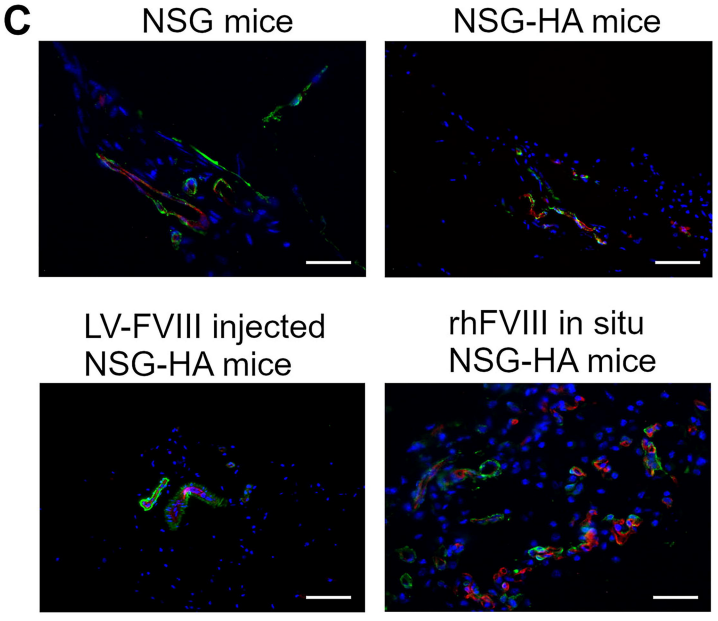
C
NSG mice
NSG-HA mice
LV-FVIII injected NSG-HA mice
rhFVIII in situ NSG-HA mice

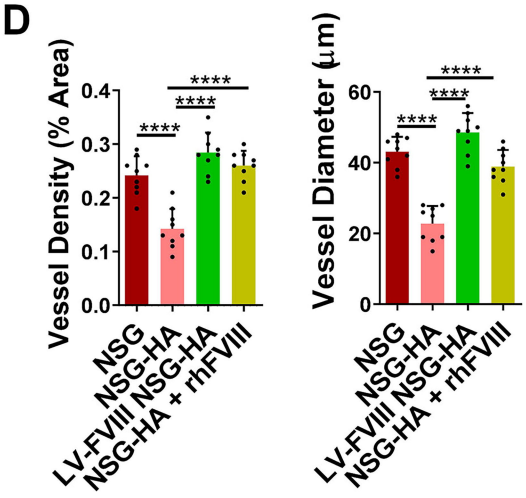
D
Vessel Density (% Area)
Vessel Diameter (µm)
NSG
NSG-HA
LV-FVIII NSG-HA
NSG-HA + rhFVIII
****

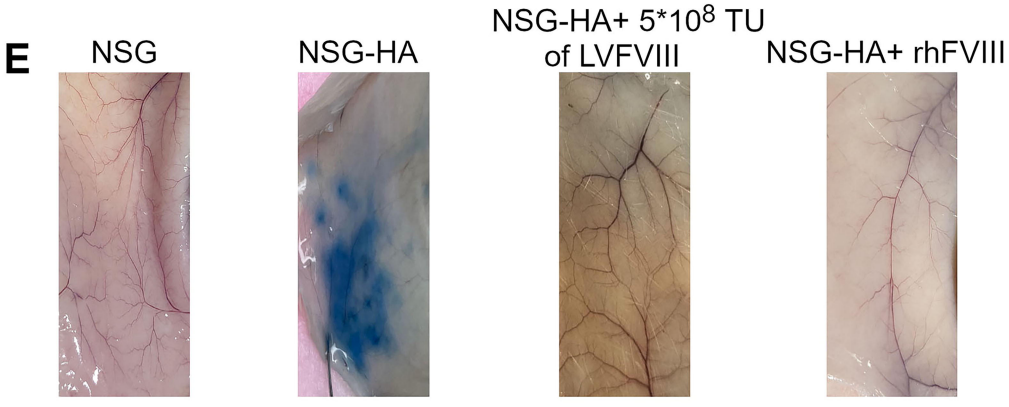
E
NSG
NSG-HA
NSG-HA+ 5*10^8 TU of LVFVIII
NSG-HA+ rhFVIII

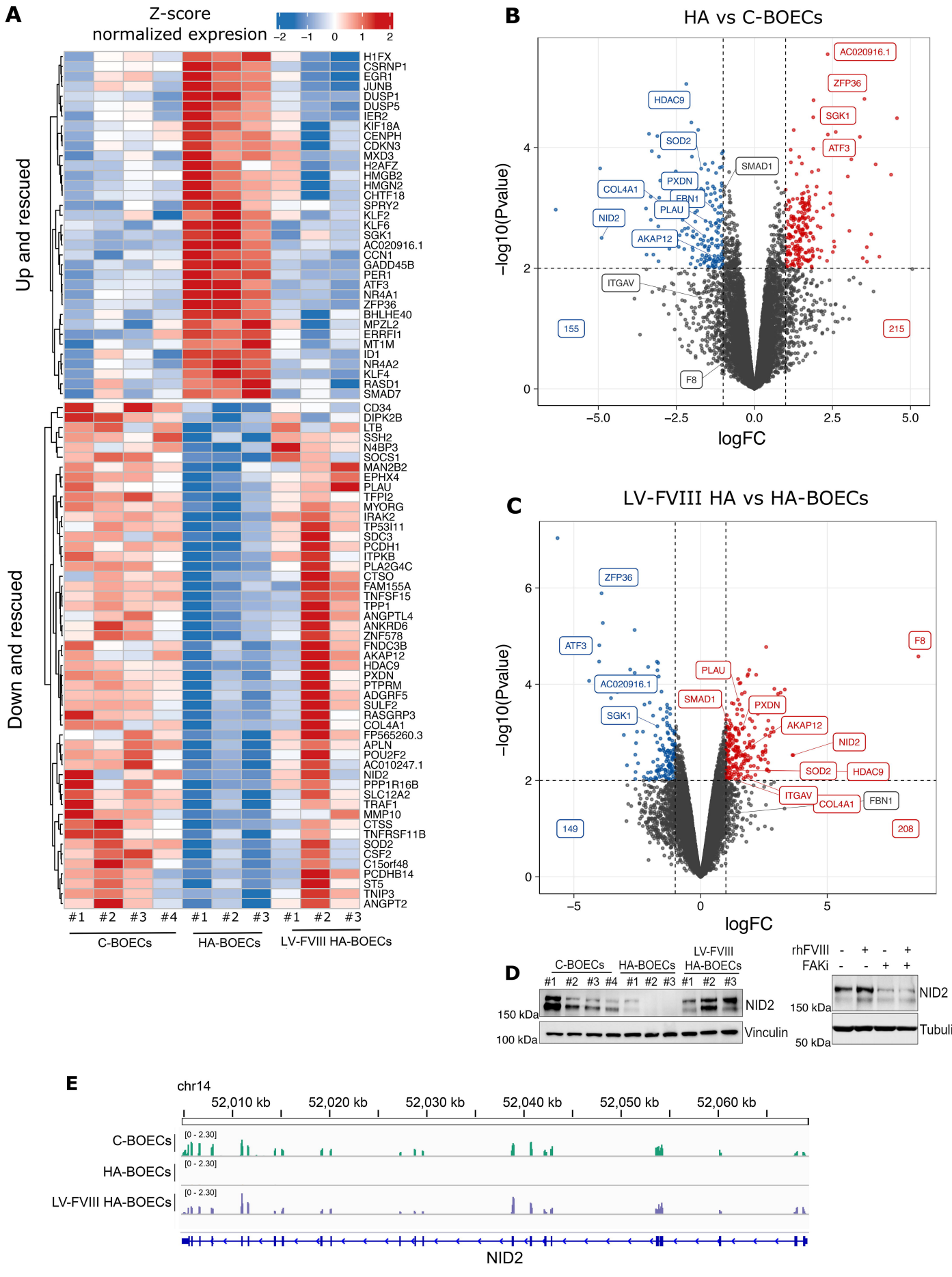
A
Z-score
normalized expresion
−2 −1 0 1 2
Up and rescued
Down and rescued
H1FX
CSRNP1
EGR1
JUNB
DUSP1
DUSP5
IER2
KIF18A
CENPH
CDKN3
MXD3
H2AFZ
HMGB2
HMGN2
CHTF18
SPRY2
KLF2
KLF6
SGK1
AC020916.1
CCN1
GADD45B
PER1
ATF3
NR4A1
ZFP36
BHLHE40
MPZL2
ERRFI1
MT1M
ID1
NR4A2
KLF4
RASD1
SMAD7
CD34
DIPK2B
LTB
SSH2
N4BP3
SOCS1
MAN2B2
EPHX4
PLAU
TFPI2
MYORG
IRAK2
TP53I11
SDC3
PCDH1
ITPKB
PLA2G4C
CTSO
FAM155A
TNFSF15
TPP1
ANGPTL4
ANKRD6
ZNF578
FNDC3B
AKAP12
HDAC9
PXDN
PTPRM
ADGRF5
SULF2
RASGRP3
COL4A1
FP565260.3
APLN
POU2F2
AC010247.1
NID2
PPP1R16B
SLC12A2
TRAF1
MMP10
CTSS
TNFRSF11B
SOD2
CSF2
C15orf48
PCDHB14
ST5
TNIP3
ANGPT2
#1 #2 #3 #4 #1 #2 #3 #1 #2 #3
C-BOECs
HA-BOECs
LV-FVIII HA-BOECs
B
HA vs C-BOECs
−log10(Pvalue)
logFC
AC020916.1
ZFP36
SGK1
ATF3
HDAC9
SOD2
SMAD1
PXDN
COL4A1
FBN1
PLAU
NID2
AKAP12
ITGAV
F8
155
215
C
LV-FVIII HA vs HA-BOECs
−log10(Pvalue)
logFC
ZFP36
ATF3
AC020916.1
SGK1
PLAU
SMAD1
PXDN
AKAP12
NID2
SOD2
HDAC9
ITGAV
COL4A1
FBN1
F8
149
208
D
C-BOECs
HA-BOECs
LV-FVIII HA-BOECs
#1 #2 #3 #4 #1 #2 #3 #1 #2 #3
150 kDa
NID2
100 kDa
Vinculin
rhFVIII - + - +
FAKi - - + +
150 kDa
NID2
50 kDa
Tubulin
E
chr14
52,010 kb
52,020 kb
52,030 kb
52,040 kb
52,050 kb
52,060 kb
C-BOECs
HA-BOECs
LV-FVIII HA-BOECs
[0 - 2.30]
NID2

Supplementary figures

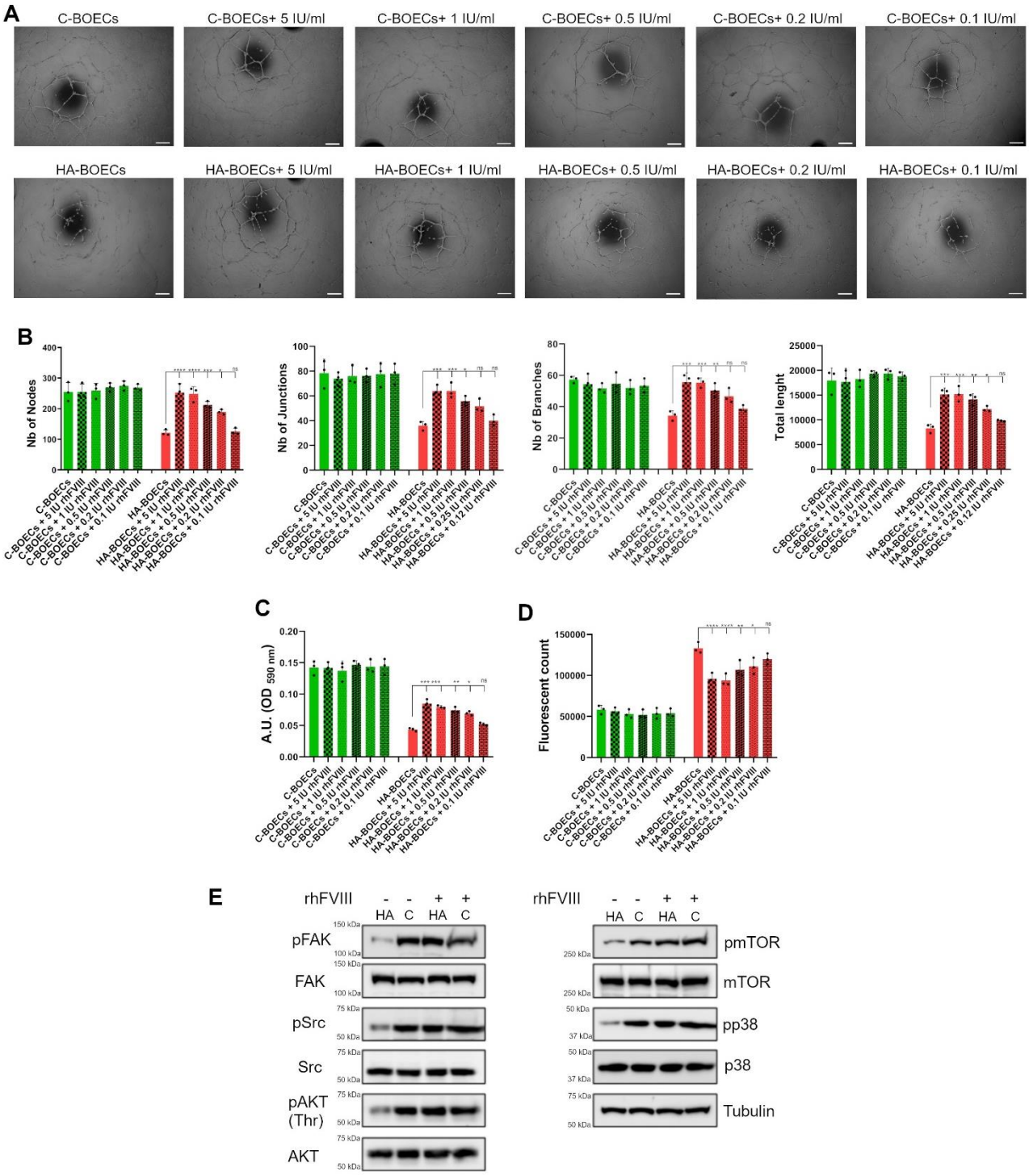

Supplementary Figure 1. Acute treatment of HA-BOECs with FVIII enhances EC functionality. A) Representative image showing the result of the tubulogenic assay on C- (n=3) and HA-BOECs (n=3) treated with 5, 1, 0.5, 0.2 and 0.1 IU/ml of B-domain-deleted rhFVIII. $5x10^4$ BOECs in culture medium with or without rhFVIII, were placed on top of the Matrigel® and incubated overnight. Scale bar = 500 µm. **B)** Quantitative analysis of the number of nodes, junctions, branches, and total length of tubule networks of cells described in **A** using ImageJ Angiogenesis software. **C)** Indirect measurement of cell migration through crystal violet

staining elution of cells described in **A**. BOECs were plated into the upper compartment of 8-μm pore size Transwell at a density of 10^5 cells in serum-free medium with or without B-domain-deleted rhFVIII, while the lower compartment was filled with complete medium and incubated overnight. After incubation, migrated cells were stained with crystal violet that was eluted with acetic acid and quantified using Victor Spectrophotometer at 590 nm. **D)** Quantification of permeability based on the extravasation of FITC-dextran through an intact monolayer of cells described in **A**. Permeability was measured across a monolayer of BOECs ($8x10^4$ cells/well) cultured on 0.1% gelatin coated Transwell (3 μm pore) with or without B-domain-deleted rhFVIII that was added every day for 1 week. At the end of the culture, 5 μg/ml of FITC-conjugated 40-kDa dextran was added to the upper chamber and the fluorescence of the lower chamber was measured in the medium using Victor Spectrophotometer (490 nm excitation/520 nm emission). Fluorescence readings were normalized to dextran permeability in transwell inserts without cells. **E)** Western blot analysis of WCL from HA- and C-BOECs treated for 15 min with or without 1 IU/ml of B-domain-deleted rhFVIII and stained with antibodies against pFAK, total FAK, pSrc, total Src, pAKT, total AKT, pmTOR, total mTOR, pp38, total p38. Tubulin was used as a loading control. Data in **B**, **C** and, **D** are expressed as mean ± SD. All experiments were performed once for each subject. Statistical analysis was performed by one-way ANOVA test (****$p < 0.0001$; ***$p < 0.001$; **$p < 0.01$; *$p < 0.05$).

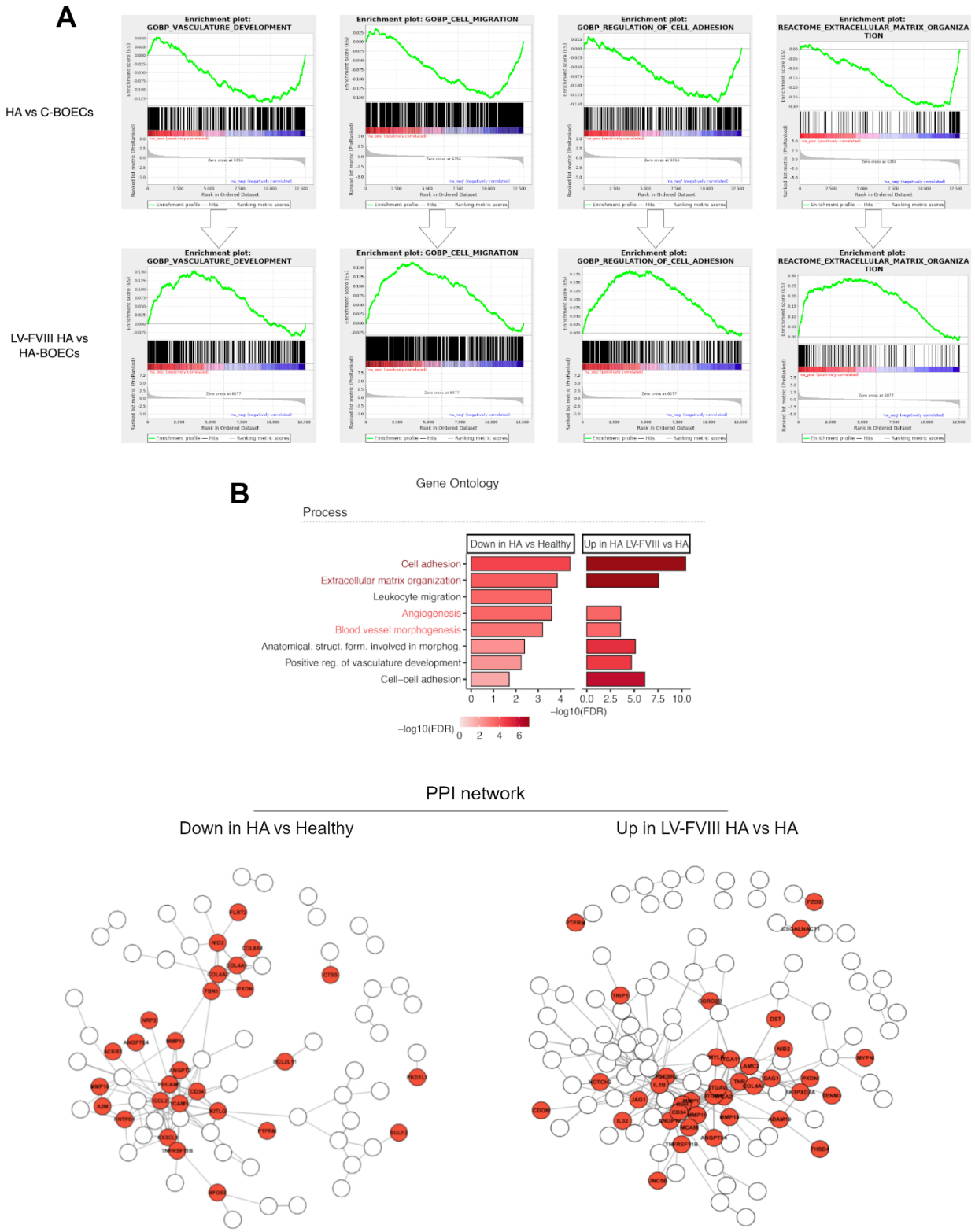

Supplementary Figure 2. GSEA and Gene Ontology analysis of FVIII-modulated genes. A) Gene set enrichment analysis (GSEA) plots depicting pathways that are downregulated in HA *vs* C-BOECs and rescued in LV-FVIII HA *vs* HA-BOECs. Key pathways include vascular development, cell migration, regulation of cell adhesion, extracellular matrix (ECM) organization and integrin cell surface interactions. Genes were considered as significantly differentially expressed (DEGs) when having |logFC| >1 and raw p value < 0.01 in

each reported comparison, as advised by SEQC consortium After the identification of a dataset of differentially expressed genes (DEGs), Enrichr online tool was used to identify pathways and gene ontology (GO) terms enriched using DEGs as input. A term is defined as significantly enriched if the reported adjusted p value is < 0.01. Gene set enrichment analysis (GSEA) was performed using a Broad Institute java package version 3.0 (classic mode) and MSigDB. **B)** On the left panel, the heatmap shows the top commonly enriched gene ontology (GO) process terms among the differentially expressed genes (DEGs) identified by RNAseq. These DEGs are compared across two categories: "Down in HA *vs* Healthy" and "Up in HA LV-FVIII *vs* HA". Hierarchical clustering was applied using the log10-adjusted *p*-values from the enrichment analysis. On the right panel, the STRING protein-protein interaction (PPI) network illustrates the interactions among these DEGs. Nodes within the network are color-coded to correspond with the commonly enriched GO annotations highlighted on the right.

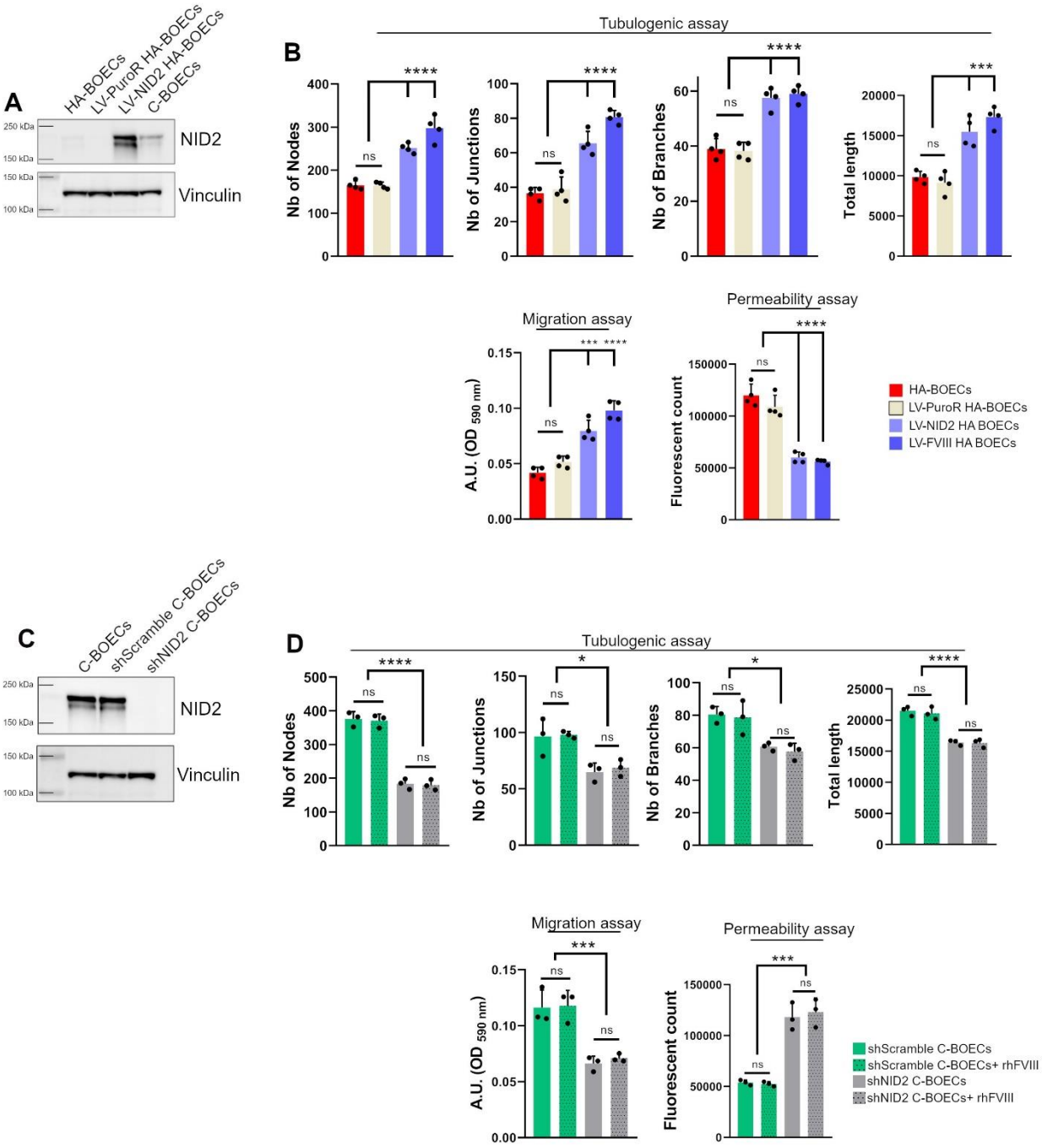

Supplementary Figure 3. NID2 expression regulates *in vitro* ECs activity. A) Western blot comparison of NID2 levels in LV-NID2 HA-BOECs *vs* HA-BOECs, with LV.PuroR HA-BOECs and C-BOECs used as controls. **B)** Quantification of number of nodes, junctions, branches, and total tubule network length in HA-BOECs and LV-PuroR, LV-NID2, and LV-FVIII HA-BOECs. LV-PuroR was used as control for LV transduction. Indirect measurement of cell migration in the BOEC groups through crystal violet staining elution. Permeability assay results, based on the extravasation of FITC-dextran through an intact monolayer in the BOEC groups, as described in **B**. **C)** Western blot analysis of NID2 expression in shNID2 C-BOECs compared to non-transduced or shScramble-transduced C-BOECs. **D)** Quantification of number of nodes, junctions, branches, and total tubule network length in shScramble C-BOECs and shNID2 C-BOECs, with or

without 1 IU/ml rhFVIII. Indirect cell migration assay results by crystal violet staining elution in the BOEC groups, as described in **B**. Permeability assay results, based on the extravasation of FITC-dextran through an intact monolayer in the BOEC groups, as described in **B**. Data in **B** and **D** are expressed as mean ± SD. All the experiments were replicated three or four times. Statistical analysis was performed by one-way ANOVA test (****$p < 0.0001$; ***$p < 0.001$ **$p < 0.01$; *$p < 0.05$).